Molecular Biology of the Cell
Vol. 21, 198–211, January 1, 2010

Growth-limiting Intracellular Metabolites in Yeast Growing under Diverse Nutrient Limitations

Viktor M. Boer,*†‡ Christopher A. Crutchfield,*§ Patrick H. Bradley,*† David Botstein,*† and Joshua D. Rabinowitz*§

*Lewis-Sigler Institute for Integrative Genomics and Departments of †Molecular Biology and §Chemistry, Princeton University, Princeton, NJ 08544

Submitted July 22, 2009; Revised October 19, 2009; Accepted October 28, 2009
Monitoring Editor: Charles Boone

Microbes tailor their growth rate to nutrient availability. Here, we measured, using liquid chromatography-mass spectrometry, >100 intracellular metabolites in steady-state cultures of *Saccharomyces cerevisiae* growing at five different rates and in each of five different limiting nutrients. In contrast to gene transcripts, where ~25% correlated with growth rate irrespective of the nature of the limiting nutrient, metabolite concentrations were highly sensitive to the limiting nutrient's identity. Nitrogen (ammonium) and carbon (glucose) limitation were characterized by low intracellular amino acid and high nucleotide levels, whereas phosphorus (phosphate) limitation resulted in the converse. Low adenylate energy charge was found selectively in phosphorus limitation, suggesting the energy charge may actually measure phosphorus availability. Particularly strong concentration responses occurred in metabolites closely linked to the limiting nutrient, e.g., glutamine in nitrogen limitation, ATP in phosphorus limitation, and pyruvate in carbon limitation. A simple but physically realistic model involving the availability of these metabolites was adequate to account for cellular growth rate. The complete data can be accessed at the interactive website http://growthrate.princeton.edu/metabolome.

INTRODUCTION

Balanced microbial growth requires the coordination of nutrient assimilation, energy generation, biosynthesis, and the cell division cycle. When nutrient availability falls to the point of impairing biosynthetic activity, microorganisms respond by decreasing their growth rate. For a nutrient-limited culture, the steady-state growth rate (μ) is a monotonic, saturable function of the extracellular concentration of the limiting nutrient ([S]) (Monod 1942), i.e.,

$$\mu = \mu_{max} * [S]/(K_s + [S]) \quad (1)$$

where K_s is the saturation constant. This relationship is best studied in chemostats, where μ can be controlled experimentally by changing the culture's dilution rate (Monod 1950; Novick and Szilard 1950; Beck and von Meyenburg, 1968; Rhee 1973; Senn *et al*., 1994). In the chemostat, in addition to "natural nutrients" (e.g., carbon, nitrogen, or phosphorus), cells also can be limited for nutrients made essential by mutations (e.g., uracil in a pyrimidine auxotroph).

The ability of cells to tailor their growth rate to a wide diversity of limiting nutrients—including auxotrophic requirements—raises the question of how cells sense nutrient availability to "know" the rate at which they can grow. Although extracellular nutrients can be sensed by receptors at the cell surface, this does not explain how cells are able to tailor their growth rate to "non-natural" nutrients required only due to mutations in biosynthetic pathways. An alternate mechanism involves sensing the extracellular nutrient based on intracellular metabolite(s). Such an approach is consistent with the ability of yeast to adjust their growth rate to both natural and auxotrophic nutrient limitations. For example, in a pyrimidine auxotroph, limitation for extracellular uracil could result in depletion of cellular UTP and CTP and thereby reduced RNA biosynthesis and slower growth.

Baker's yeast, as the best-studied eukaryotic microbe, provides a valuable system for investigating the pathways linking nutrient environment to growth rate. Recent studies have examined the transcriptome (and to a limited extent, the proteome and secreted metabolites) of nutrient-limited yeast cultures (Gasch *et al*., 2000; Boer *et al*., 2003; Kolkman *et al*., 2006; Castrillo *et al*., 2007; Brauer *et al*., 2008; Pir *et al*., 2008). This research has revealed close ties between the transcriptome and growth rate. Expression of more than a quarter of genes in yeast depends strongly on growth rate, in a manner insensitive to which nutrient limits growth (Brauer *et al*., 2008). The mechanisms linking the nutrient environment to transcription and growth rate, however, have remained unclear.

To investigate such mechanisms, here we use liquid chromatography-tandem mass spectrometry (LC-MS/MS) to measure the intracellular metabolome of yeast limited for five different nutrients (glucose as the sole carbon source, ammonium as the sole nitrogen source, phosphate as the sole phosphorus source, uracil, and leucine), with each limiting nutrient tested at five different growth rates. The experimental design and the physiological circumstances in the chemostats parallel those in which the transcript measurements had been made previously (Brauer *et al*., 2008).

This article was published online ahead of print in *MBC in Press* (http://www.molbiolcell.org/cgi/doi/10.1091/mbc.E09–07–0597) on November 4, 2009.

‡ Present address: DSM Food Specialties, Alexander Fleminglaan 1, 2613 AX Delft, The Netherlands.

Address correspondence to: Joshua D. Rabinowitz (joshr@princeton.edu).

Consistent with its close link to the nutrient environment, we find that the intracellular metabolome varies greatly depending on the identity of the limiting nutrient and the severity of nutrient limitation. Unlike gene transcripts, there are only a limited number of metabolites whose abundance shows a correlation with growth rate independent of the limiting external nutrient. Different limiting nutrients cause the intracellular concentrations of distinct classes of metabolites to decrease. Nitrogen limitation is associated with low intracellular levels of amino acids, especially glutamine and its products. Phosphorus limitation is associated with low levels of a broad spectrum of phosphorylated compounds, including ATP. Strikingly, phosphorus limitation produces a much lower "adenylate energy charge" than carbon (glucose) limitation. Thus, energy charge also measures "phosphorus charge."

To begin to quantitatively define possible pathways linking nutrient availability to growth, we develop statistical criteria for metabolites that may potentially serve as intracellular species limiting growth. We show that metabolites meeting these criteria include glutamine for nitrogen limitation, ATP for phosphorus limitation, pyruvate for carbon (glucose) limitation, and UTP for uracil limitation. We further develop a simple steady-state model in which growth rate depends on the availability of these four intracellular compounds.

MATERIALS AND METHODS

Strains and Cultivation

Saccharomyces cerevisiae was cultivated in chemostats using five different limiting nutrients, each at five different dilution rates (~0.05, 0.11, 0.16, 0.22 and 0.30 h^{-1}). Three isogenic FY derivative strains (Winston *et al*., 1995) were used: for carbon, nitrogen, and phosphorus limitation, the prototrophic strain DBY11069 (*MATa*); for leucine limitation, the leucine auxotroph DBY11167 (*MATa leu2Δ1*); and for uracil limitation, the uracil auxotroph DBY7284 (*MATa ura3-52*).

A single colony was grown overnight in batch in 3 ml of mineral medium before inoculation (0.5–1 ml) of the chemostat. The duration of the batch phase in the chemostat was between 16 and 24 h, depending on the density. Media composition was adapted from Brauer *et al*. (2008) and can be found in Supplemental Table S4. All media were filter sterilized through a 0.22-μm pore filter (Steritop; Millipore, Billerica, MA).

Cultures were grown in continuous mode in 500-ml chemostats (Sixfors; Infors AG, Bottmingen, Switzerland), with a working volume of 300 ml. Cultures were stirred at 400 rpm, sparged with five standard liters per minute of humidified air, and maintained at pH 5.0 with the automatic addition of 0.1 or 0.2 M KOH. Cultures were routinely monitored for culture density (Klett), cell count, and mean cell size (Z2 cell and particle counter; Beckman Coulter, Fullerton, CA). All samples for metabolite and biomass analysis were taken during two consecutive days of steady-state growth.

Sampling and Extraction of Intracellular Metabolites

Each chemostat was sampled for metabolites four times over the course of 2 d. In parallel with each sampling of the experimental chemostats, two independent phosphorus-limited chemostats (D = 0.05 h^{-1}) were sampled as an external reference to correct for day-to-day variation in the LC-MS/MS analysis as described below. Two sampling methods were performed, each once per day:

Methanol Quenching Method. Ten milliliters of culture broth was directly quenched in 20 ml of −80°C methanol and centrifuged for 5 min at 4000 rpm in a −80°C pre-chilled rotor (JA-25.50; Beckman Coulter) in a −10°C centrifuge. Supernatant was discarded, and 0.4 ml of −20°C extraction solvent (acetonitrile:methanol:water, 40:40:20) was added to the pellet (Rabinowitz and Kimball, 2007). The pellet was extracted for 15 min at 4°C, the suspension was centrifuged, and the supernatant set aside. The pellet was extracted again at 4°C with 0.4 ml of extraction solvent for 15 min, the suspension was again centrifuged, and the supernatants were pooled (total extraction volume, 0.8 ml).

Vacuum Filtering Method. Ten milliliters of culture broth was rapidly sampled from the chemostat and vacuum filtered over a 0.45-μm pore size, 25-mm nylon filter (Millipore), and the filter was immediately quenched in 0.6 ml of −20°C extraction solvent. After 15 min at −20°C, the cell material was mixed into the extraction solvent, the filter was washed with an additional 0.1 ml of extraction solvent, the resulting suspension was centrifuged at 4°C, and the supernatant set aside. The pellet was extracted again with 0.1 ml of extraction solvent for 15 min at 4°C, the suspension was again centrifuged, and the supernatants were pooled (total extraction volume, 0.8 ml). Filtrates from the vacuum filtering were used for glucose and ethanol determination, as described previously (Brauer *et al*., 2008).

LC-MS/MS Analysis

Cell extracts were analyzed using liquid chromatography-electrospray ionization-triple quadrupole mass spectrometry in multiple reaction monitoring (MRM) mode. Positive ionization mode analysis was on a Quantum Ultra triple quadrupole mass spectrometer (Thermo Electron, San Jose, CA), coupled to hydrophilic interaction chromatography on an aminopropyl stationary phase (for details of the LC method and MRM scans, see Bajad *et al*., 2006). Negative ionization mode analysis was on a Finnigan TSQ Quantum DiscoveryMax triple quadrupole mass spectrometer (Thermo Electron) coupled to tributylamine ion-pairing reversed phase chromatography on a C18 stationary phase (a variant of the method of Luo *et al*., 2007, modified as described in Lu *et al*., 2008). Autosampler temperature was 4°C and injection volume was 10 μl.

For routine quality control, isotope-labeled standards of ten metabolites (e.g., ATP, glutamine, glutamate) were spiked into the extracts. Isotope-labeled leucine and uracil were used for quantitation of their extracellular concentrations.

To determine the absolute intracellular concentrations of ATP, ADP, and AMP (as required to measure adenylate energy charge), isotope-labeled ATP, ADP, and AMP were spiked into the extraction solvent before extraction of two phosphate-limited chemostats (D = 0.05 h^{-1}). Absolute concentrations were then determined using a mass ratio-based approach (Wu *et al*., 2005; Bennett *et al*., 2008). Absolute concentrations in other conditions were then determined by comparison with the measured absolute concentration in the phosphorus-limited reference condition.

Normalization and Clustering

To convert raw LC-MS/MS ion counts to relative cellular concentration data, ion counts were first normalized by the total cell volume extracted and the volume of the extraction solvent, as follows:

$$\text{Normalized ion counts} = \text{Raw ion counts} \times (\text{cell count/ml culture})^{-1}$$

$$\times (\text{mean cell volume})^{-1} \times (\text{ml culture extracted})^{-1} \times (\text{ml extraction solvent})$$

Cell count per milliliter and mean cell volume were determined based on electrical impedance by Coulter counter (for measurements, see Supplemental Table S3). Cell counts are reported in units of 10^7 cells/ml; mean cell volume is reported in picoliters. A typical calculation is as follows: normalized ion counts = 5000 raw ion counts $\times$ $(2)^{-1}$ $(10^7$ cells/ml$)^{-1} \times 0.03^{-1}$ (pl/cell)$^{-1} \times$ 10^{-1} (ml cultured extracted)$^{-1} \times$ (0.8) (ml extraction solvent) = 6667 normalized ion counts.

Normalization factors (the ratio of raw ion counts to normalized ion counts) varied from 0.38 to 2.1. After normalization, absent values (where no peak was detected) and normalized ion counts below 300 were set to 300 to remove variation in compounds that were near the limit of detection. The selection of 300 normalized ion counts as a floor value is based on the lower limit of quantitation typically being ~100 ion counts and the smallest normalization factor being 0.38. Normalized ion counts for each metabolite in every sample are provided in Supplemental Dataset 2.

Normalized ion counts were then converted to relative concentrations by dividing the value for the experimental samples by the corresponding value from the phosphorus-limited reference chemostat (matched for date of analysis and methanol quenching or vacuum filtration):

$$\text{Relative concentration} = \text{Normalized ion counts}_{\text{experimental sample}}$$

$$\times (\text{Normalized ion counts}_{\text{phosphorus limited reference}})^{-1}$$

Because each experimental chemostat was sampled four times, and each experimental sample was paired to two independent phosphorus-limited reference samples, this gave eight values for each condition. The median and interquartile range of these eight values (reflective of four independent samples from a single chemostat) was used for further analysis.

For heat map display, relative concentrations were $\log_2$ transformed and mean centered over all conditions (i.e., growth rates and nutrient limitations). The data were then hierarchically clustered by metabolite using Pearson correlation (Eisen *et al*., 1998). The mean-centered, $\log_2$-transformed data used to generate Figure 1 are provided as Supplemental Table S5.

Statistical Determination of Growth Rate Slopes and Nutrient Mean Effects

Data were fit to Eq. 2 using the R statistical software package (R Development Core Team, 2008) to obtain estimates of each parameter value and its associ-

ated SE. A *t*-statistic was then calculated by taking the ratio of the estimated value and its SE. This *t*-statistic was used to test whether the value of the parameter was significantly different from 0. The resulting p values were then corrected for multiple hypothesis testing via the false discovery rate (FDR) procedure of Benjamini and Hochberg (1995).

Modeling of Cellular Growth

Cellular growth was modeled as the assembly of a polymer requiring four limiting intracellular metabolites, according to Eq. 5. In this equation, the nutrient limitation is denoted by $n \in \{C, N, P, U\}$. x_n is a normalized measure of the concentration of a particular candidate limiting nutrient: specifically, $x_n = 2^{y_n}$, where y_n represents the mean-centered $\log_2$(fold-change) for pyruvate (n = *C*), glutamine (n = *N*), ATP (n = *P*), or UTP (n = *U*). μ_{max} represents the growth rate when all essential nutrients are abundant, and the k_n terms represent the Michaelis constants for the compounds whose concentrations are given by the x_n. Leucine limitation was not included in the above-mentioned model because leucyl-tRNA, the likely limiting molecular species, was not measured in the current study.

To assess goodness-of-fit, we used leave-one-out cross-validation, in which 19 of the 20 available data points (4 nutrient limitations at 5 growth rates each) were used to learn the parameters for the model. This model was then used to predict the growth rate only for the remaining condition. In this way, a predicted value was obtained for each of the 20 possible data points. The squared Pearson r between the predicted and the known values for μ was 0.78 ($p = 3 \times 10^{-7}$), indicating robust agreement between the model output and the actual growth rate. The nonlinear R^2, which provides another measure of goodness of fit, was found to be 0.75, as measured by the following formula:

$$R^2 = 1 - \frac{SS_{res}}{SS_{tot}}$$

SS_{res} here refers to the sum of squares of the residual (i.e., the known values minus the predicted values), whereas SS_{tot} refers to the sum of squares of the mean-subtracted known values.

RESULTS AND DISCUSSION

We used LC-MS/MS to analyze >180 compounds, representing a substantial fraction of the >600 compounds of the known yeast metabolome (Herrgård *et al*., 2008). Of the analyzed compounds, reliable relative quantitation (i.e., fold change across biological conditions), was obtained for ~100 of these (see Supplemental Table S1). These compounds include most central carbon metabolites, amino acids, and nucleotides.

Intracellular metabolites were extracted from chemostat cultures using two methods. One involved mixing culture medium containing cells directly into cold methanol, followed by isolation of the cells by centrifugation and subsequent extraction of the cell pellet (de Koning and van Dam 1992). The other involved isolation of the cells by vacuum filtration followed by quenching and extraction of the filter-trapped cells. In both methods, acetonitrile:methanol:water (40:40:20) was used as the extraction solvent, as for most compounds it gave equal or greater yields to methanol:water (the previous literature standard; Maharjan and Ferenci 2003; Villas-Bôas *et al*., 2005). In particular, acetonitrile:methanol:water was substantially more effective at extracting nucleotides from filter-trapped cells (Supplemental Figure S1A and Supplemental Table S2). Although the filtration method gave larger absolute signals for nucleotide triphosphates (Supplemental Figure S1B), relative metabolite concentration changes across biological samples (i.e., mass spectrometry signals normalized to the volume of the extracted cells and then to the geometric mean across all chemostat conditions) were robust to the sampling method (Supplemental Figure S2). Because both methods gave comparable relative quantitation, the data were pooled in all subsequent analysis. A complete summary of the pooled data, expressed as $\log_2$ ratios of the relative metabolite concentration changes, is provided in Supplemental Dataset 1. Similar data clustering and quantitative conclusions are obtained from independent analysis of either the methanol-quenched cells or the vacuum-filtered cells.

Whole Metabolome View

We used hierarchical clustering (Pearson correlation; Eisen *et al*., 1998) of the metabolites to view the relative differences and similarities in metabolite concentrations among conditions (Figure 1, for alternative color scheme see Supplemental Figure S2). This display suggests several general conclusions. First, metabolites belonging to the same class, such as pyrimidine intermediates, amino acids, or tricarboxylic acid (TCA)-cycle intermediates, formed remarkably consistent clusters. Second, the levels of almost all metabolites depended strongly on the identity of the limiting nutrient, with profound differences across conditions that for several compounds even exceeded 100-fold. Third, the differences between nutrients were most pronounced at the slowest growth rate, at which the limitation was most stringent.

Although the concentrations of only a few measured metabolites correlated with growth rate regardless of the nature of the nutrient limitation, within each particular nutrient limitation, many metabolite levels did change consistently with respect to the growth rate. Generally, the compounds that showed the strongest growth rate effect were directly related to the limiting nutrient. For example, most amino acids were depleted in nitrogen limitation, especially at slow growth rates, and rose with increasing growth rate. Similarly, nucleotide triphosphates were depleted in phosphorus limitation and rose with faster growth rate. The inverse was true for nitrogenous bases and nucleosides, whose concentrations were elevated in phosphorus limitation and declined with faster growth rate. The general trend toward amino acid depletion in nitrogen limitation and nucleotide triphosphate depletion in phosphorus limitation is consistent with previous literature showing that nitrogen limitation restricts protein synthesis and that phosphorus limitation restricts nucleic acid synthesis in *Enterobacter aerogenes* (Cooney and Wang 1976).

Identification of Growth-limiting Intracellular Metabolites

As a prelude to searching for intracellular metabolites that might limit growth, we confirmed that the growth rate was related to the extracellular concentration of the limiting nutrient. As expected, growth rate was a monotonic function of the concentration of the limiting nutrient, as shown for glucose, uracil, and leucine limitation in Supplemental Figure S3. The estimated values for μ_{max} (Supplemental Figure S3), derived from the Michaelis–Menten relationship (Eq. 1), approximate the empirically observed maximum growth rate in exponential batch culture (Pronk 2002).

For depletion of an intracellular metabolite to limit growth, we reasoned that its concentration must 1) be uniquely low in the nutrient condition where it is growth-limiting; and 2) within that condition, rise when the limitation is partially relieved, i.e., with increasing growth rate. In each limitation regime, we identified several metabolites that qualitatively met these criteria. Some examples include glutamine, a central nitrogen assimilation metabolite, in nitrogen limitation; ATP, the free energy currency and RNA building block, in phosphorus limitation; pyruvate, the glycolytic end product, in carbon (glucose) limitation; and UTP, the RNA building block, in uracil limitation. These four examples are illustrated in Figure 2. In each case, there is a well-understood connection between the limiting nutrient and the potentially growth-limiting intracellular metabolite.

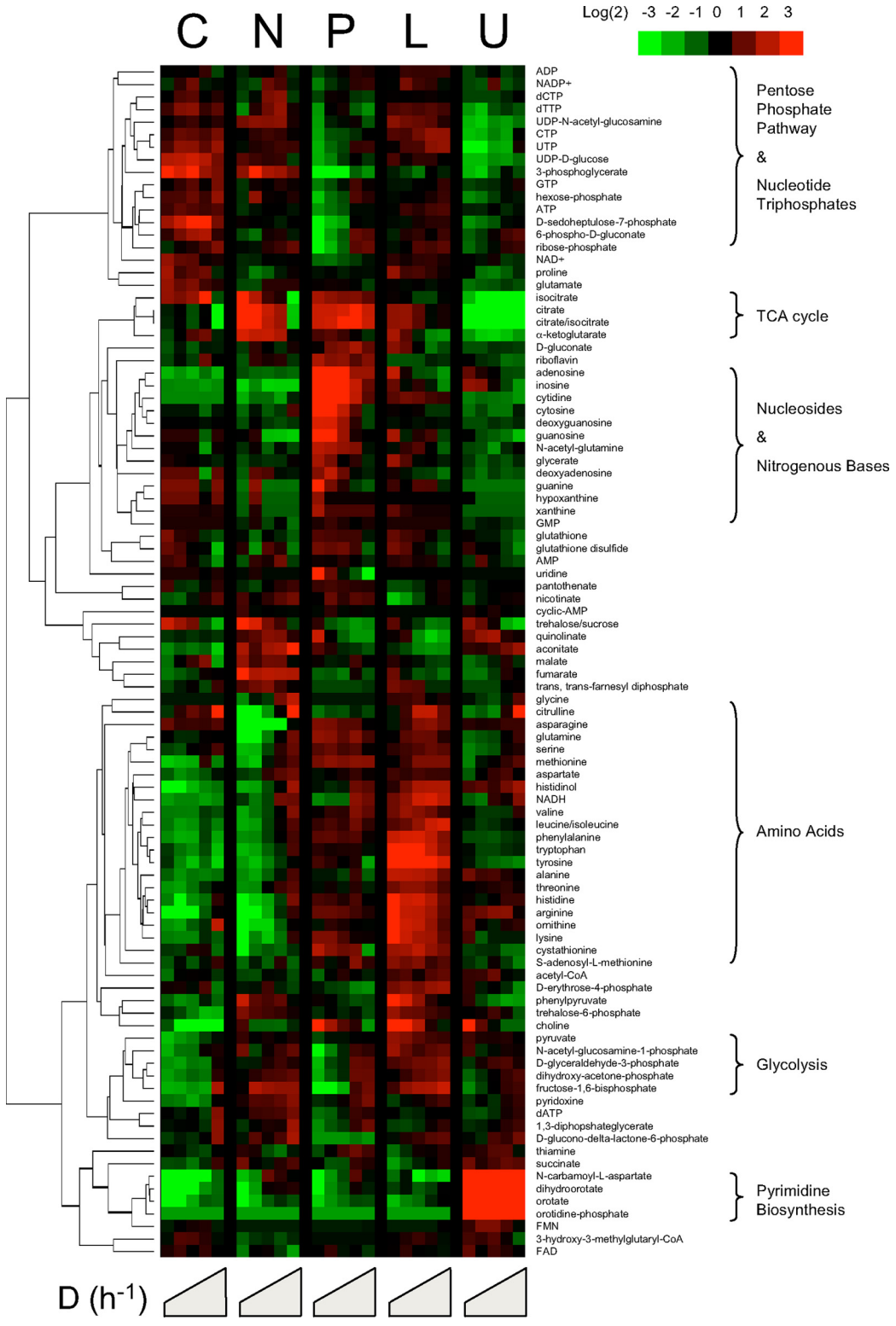

Figure 1. Clustered heat map of yeast metabolome variation as a function of growth rate and identity of the limiting nutrient. Rows represent specific intracellular metabolites. Columns represent different chemostat dilution rates (equivalent to steady-state cellular growth rates) for different limiting nutrients (C, limitation for the carbon source, glucose; N, limitation for the nitrogen source, ammonium; P, limitation for the phosphorus source, phosphate; L, limitation for leucine in a leucine auxotroph; U, limitation for uracil in a uracil auxotroph). Plotted metabolite levels are $\log_2$-transformed ratios of the measured sample concentration to the geometric mean concentration of the metabolite across all conditions. Data for each metabolite is mean-centered, such that the average $\log_2$(fold-change) across all samples is 0. Dilution rates increase within each condition from left to right from 0.05 to 0.3 h^{-1}. Plotted values are the median of N = 4 independent samples from each chemostat.

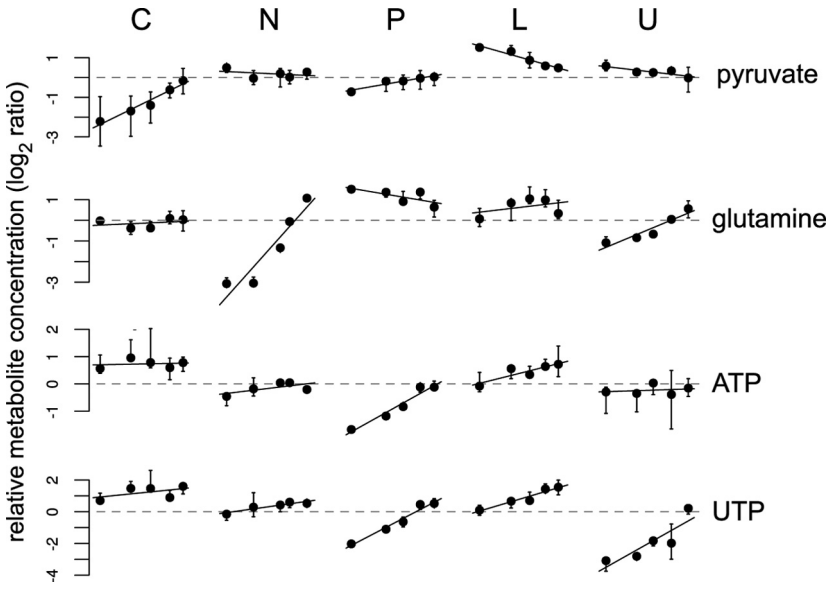

Figure 2. Examples of metabolites that are potentially limiting growth under glucose limitation, ammonium limitation, phosphate limitation, and uracil limitation (from top to bottom). Metabolite concentrations are plotted on a $\log_2$ scale and mean-centered as per Figure 1. Values represent the median (black circles) and interquartile range (bars) of N = 4 independent samples from each chemostat. For a given limiting nutrient, steady-state growth rate increases from left to right from 0.05 to 0.3 h^{-1}. Limiting nutrients are as per Figure 1: C, limitation for the carbon source, glucose; N, limitation for the nitrogen source, ammonium; P, limitation for the phosphorus source, phosphate; L, limitation for leucine in a leucine auxotroph; U, limitation for uracil in a uracil auxotroph. Trend lines are a fit to the linear model described in Figure 3.

To systematically identify the full set of potential growth-limiting metabolites, we quantitatively assessed the impact of nutrient condition and growth rate on intracellular metabolite concentrations. The data for each metabolite–nutrient condition pair were fit to the following simple model:

$$\log([M]_{n,\mu}/[M]_o) = m_n \log(\mu/\mu_o) + b_n \quad (2)$$

where $[M]_{n,\mu}$ is the metabolite's concentration in yeast growing at rate μ with limiting nutrient n, $[M]_0$ is the geometric mean concentration of the metabolite across all conditions, μ is the growth rate, μ_0 is the geometric mean growth rate, and m_n and b_n are model parameters (see Figure 3 for an illustration of the model). The parameter b_n (the "nutrient mean effect") captures whether limitation for nutrient n generally enhances or depletes the metabolite M. The parameter m_n (the "growth rate slope") captures the effect of growth rate within that nutrient limitation, i.e., whether [M] increases or decreases when the nutrient limitation is partially relieved and growth rate rises. Although used here primarily as a statistical tool, Eq. 2 also approximates typical functions used to relate metabolite concentrations and growth rate in cells. For example, if growth rate is a saturable function of the concentration of a limiting metabolite M as per Eq. 1, then the slope m_n in Eq. 2 is the inverse of the Hill coefficient of the function in the growth-limited regime (see Supplemental Material derivation of this relationship).

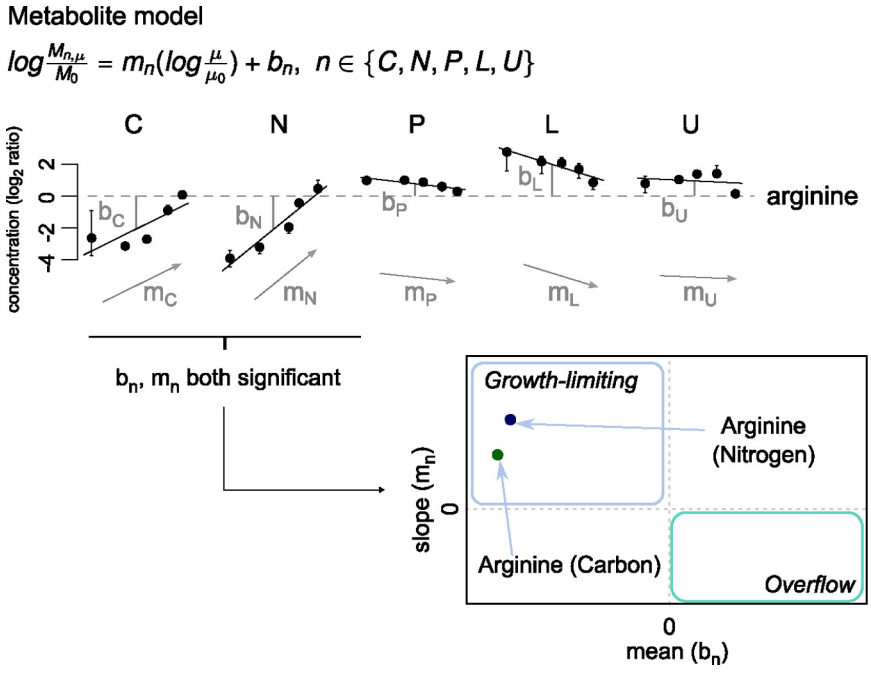

Figure 3. Model-based determination of the nutrient mean effect and growth rate slope, using arginine as an example metabolite. Arginine concentration data (plotted using the same conventions as in Figure 2) were fit to Eq. 2; b_n is the nutrient mean effect and m_n is the growth rate slope. Units of the nutrient mean effect are $\log_2$(fold-change) and of the growth rate slope are $\log_2$(fold-change)/(growth rate). For example, a nutrient mean effect of −2 (as found for arginine in glucose limitation) implies that the average arginine concentration in glucose limitation is one-quarter (i.e., 2^{-2}) the overall average. Once growth rate slope and nutrient mean effects are calculated, they can be plotted against each other (bottom right). Candidate growth-limiting metabolites have a negative nutrient mean effect and a positive growth rate slope, and accordingly fall in the top left quadrant. Overflow metabolites have a positive nutrient mean effect and negative growth rate slope, and accordingly fall in the bottom right quadrant. Compound-nutrient pairs are plotted when the nutrient mean effect and growth rate slope are both significant at FDR <0.1. For arginine, this occurred in nitrogen limitation and in carbon limitation but not in the other nutrient conditions. In both nitrogen limitation and carbon limitation, arginine showed a growth-limiting pattern.

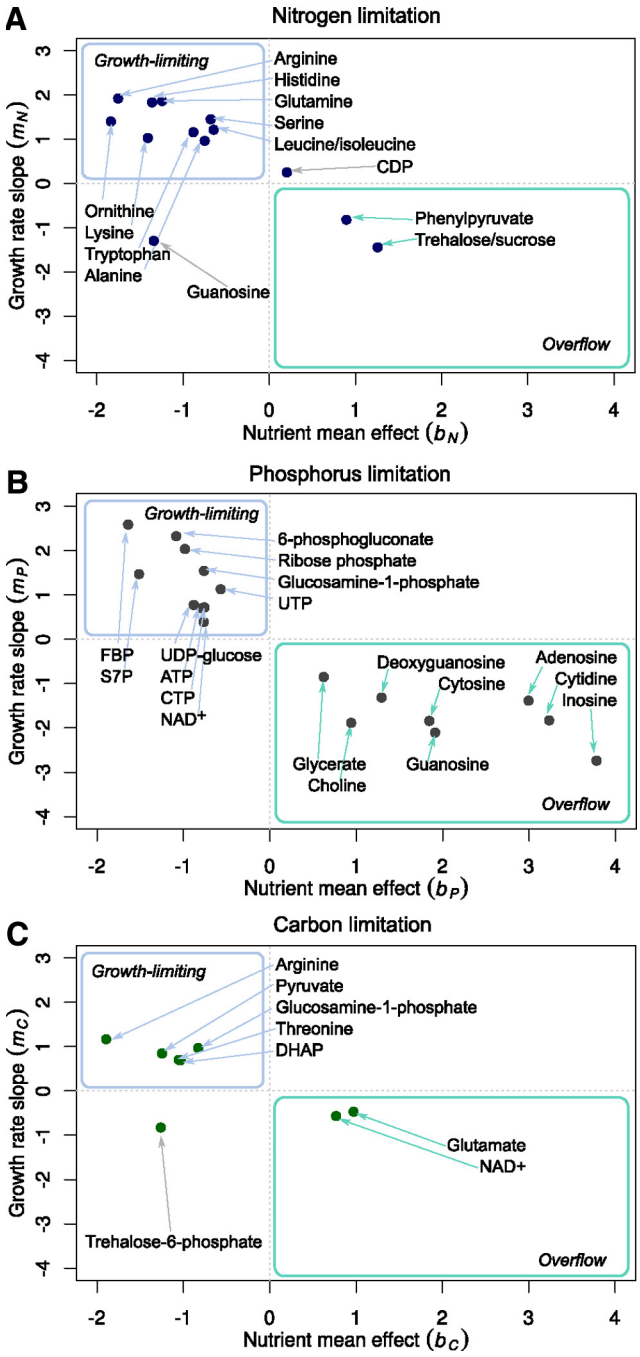

Figure 4. Growth-limiting and overflow metabolites. Data for all metabolites were fit to the model exemplified in Figure 3. Resulting plots of growth rate slope versus nutrient mean effect are shown here. (A) Nitrogen (ammonium) limitation. (B) Phosphorus (phosphate) limitation. (C) Carbon (glucose) limitation. For all plotted metabolites, both the growth rate slope and nutrient mean effect were significant (FDR <0.1). In each plot, candidate growth-limiting metabolites are found in the upper left quadrant, and overflow metabolites in the lower right quadrant.

Figure 4 plots nutrient mean effects versus growth rate slopes for various metabolites in nitrogen, phosphorus, and carbon (glucose) limitation, respectively. The metabolites shown are those with statistically significant effects on both dimensions at an FDR of 0.1. Supplemental Figure S4 shows analogous data for the auxotrophic limitations. These plots are also available in an interactive format on the website at http://growthrate.princeton.edu/metabolome/.

For each nutrient condition, candidate growth-limiting species were those with relatively low concentrations (negative nutrient mean effect) that rose with growth rate (positive growth rate slope). Such metabolites are found in the upper left quadrant of the plots in Figure 4, with roughly 10 candidates found per natural limitation. In contrast, for uracil limitation, we found only three candidates, two of which were UTP and CTP, the biopolymer precursors most directly linked to pyrimidine auxotrophy (Supplemental Figure S4). The identification of UTP and CTP in uracil limitation supports the validity of the analytical method. For leucine limitation, the analysis was less informative, as we were unable to resolve leucine from its structural isomer, isoleucine, in the present LC-MS/MS method.

In addition to identifying candidate growth-limiting metabolites, Eq. 2 also identified compounds that increase in response to limitation for a particular nutrient. Such "overflow metabolites" are characterized by a positive nutrient mean effect and negative growth rate slope and are found in the lower right quadrant of the plots in Figure 4. Although somewhat fewer "overflow" than "growth-limiting" species were found, those identified tended to be clearly related to the nutrient limitation and often lacked the limiting element, e.g., nucleosides and nitrogenous bases in phosphorus limitation.

It should be noted that the nutrient mean effect term of the linear model can be skewed by metabolites that are extreme in one condition. For example, pyrimidine intermediates accumulated so greatly in the uracil auxotroph that their concentrations in all other conditions were significantly below the overall mean, i.e., a strong positive nutrient mean effect in uracil limitation resulted in the "artifactual" appearance of a negative nutrient mean effect in the other conditions. To avoid such skewing due to the auxotrophs, we repeated the above-mentioned analyses using only data for carbon, nitrogen, and phosphorus limitation (the natural limitations). With the exception of pyrimidine intermediates (which are omitted from Figure 4 on this basis), the results were qualitatively the same; however, due to smaller dataset size, statistical significance of some effects was reduced. For plots using only the natural limitation data, see Supplemental Figure S5 or http://growthrate.princeton.edu/metabolome/.

As one approach to identify particularly interesting potential growth-limiting metabolites, for each nutrient limitation, we ordered the metabolites by statistical significance, first considering only the nutrient mean effect and then considering only the growth rate slope. Metabolites were then prioritized based on the sum of their ranks in these two dimensions (Table 1). This prioritization, based on statistical significance, favors metabolites that both fit the model closely and have strong nutrient mean effects and growth rate slopes. For example, in carbon (glucose) limitation, although arginine has the strongest nutrient mean effect and growth rate slope (Figure 4C), pyruvate better fits the model, rising more steadily with increasing growth rate (compare carbon limitation data in Figures 2 and 3), and accordingly rises to the top of Table 1.

Growth-limiting Species in Nitrogen (Ammonium) Limitation

A large cluster of amino acids were decreased in nitrogen limitation (Figure 1). Amino acids are logical candidates for limiting cellular growth. For example, low amino acid levels could limit the rate of tRNA charging. This in turn could

Table 1. Candidate growth-limiting metabolites under carbon, nitrogen, phosphorus, leucine, and uracil limitation

Limiting nutrient	Name	b_n p value	m_n p value	Rank sum
Glucose	Pyruvate	1×10^{-8}	7×10^{-5}	2
	Dihydroxyacetone-phosphate	8×10^{-5}	3×10^{-2}	4
	Threonine	1×10^{-4}	5×10^{-2}	7
	Arginine	1×10^{-4}	7×10^{-2}	7
	N-Acetyl-glucosamine-1-phosphate	4×10^{-2}	8×10^{-2}	10
Ammonium	Glutamine	5×10^{-4}	3×10^{-4}	5
	Arginine	3×10^{-4}	2×10^{-3}	5
	Serine	9×10^{-3}	3×10^{-4}	8
	Ornithine	4×10^{-4}	5×10^{-2}	9
	Leucine/isoleucine	2×10^{-2}	2×10^{-3}	11
	Tryptophan	5×10^{-3}	6×10^{-3}	11
	Histidine	6×10^{-3}	7×10^{-3}	11
	Lysine	9×10^{-4}	1×10^{-1}	13
	Alanine	3×10^{-2}	5×10^{-2}	17
Phosphate	ATP	8×10^{-6}	8×10^{-4}	4
	Ribose-phosphate	3×10^{-5}	5×10^{-7}	4
	D-Sedoheptulose-7-phosphate	1×10^{-4}	2×10^{-3}	9
	6-Phospho-D-gluconate	5×10^{-3}	1×10^{-4}	9
	NAD^+	2×10^{-5}	7×10^{-2}	12
	Fructose-1,6-bisphosphate	6×10^{-3}	2×10^{-3}	12
	UDP-D-glucose	1×10^{-3}	3×10^{-2}	13
	N-Acetyl-glucosamine-1-phosphate	7×10^{-2}	3×10^{-3}	15
	CTP	5×10^{-3}	6×10^{-2}	15
	UTP	1×10^{-1}	8×10^{-3}	17
Leucine	Nicotinate	8×10^{-4}	1×10^{-3}	2
Uracil	UTP	3×10^{-6}	4×10^{-3}	2
	CTP	8×10^{-6}	5×10^{-2}	5
	Serine	5×10^{-2}	3×10^{-2}	5

As in Eq. 2, b_n refers to the nutrient mean effect (i.e., displacement from the overall mean), whereas m_n refers to the growth-rate slope under a particular limitation condition. For an illustration of the model, see Figure 3. Here, we present only those metabolites with b_n significantly >0 and m_n significantly <0 (FDR <0.1). Within a nutrient limitation, the FDR-adjusted p values for both parameters (columns 3 and 4) were ranked separately, and these ranks were added to give the rank sum in column 5. This rank sum was then used to order the metabolites.

lead to the accumulation of uncharged tRNA and impaired protein synthesis.

Every compound identified as potentially growth limiting in ammonium limitation was an amino acid (Figure 4A, top left quadrant). Amino acids are linked to ammonium via glutamine (produced by reaction of ammonia with glutamate) or glutamate (produced by reaction of ammonia with α-ketoglutarate). Glutamine, but not glutamate, was identified as potentially growth-limiting. The growth-limiting pattern of glutamine was strong, highest in the ranked list of metabolites depleted in nitrogen limitation (Table 1). In addition, three of the four proteinogenic amino acids receiving nitrogen from glutamine (arginine, histidine, and tryptophan) were identified as potentially growth limiting (the fourth, asparagine, just missed the cut-off for statistical significance). Interestingly, nucleotides, which are also products of glutamine, were not similarly decreased.

Examination of the growth rate slope across all amino acids revealed that the concentration of every amino acid dropped with increasingly severe ammonium limitation, with the strongest response for glutamine, histidine and arginine, which contain two, three, and four nitrogens, respectively (Figure 5). Both arginine and histidine receive nitrogen from glutamine, further implicating glutamine in control of nitrogen-limited growth.

Glutamine is preferred among amino acids as a nitrogen source for *Saccharomyces*. Moreover, genetic or pharmacological inhibition of glutamine synthesis induces transcription of nitrogen-responsive genes (Mitchell and Magasanik 1984; Crespo *et al*., 2002; Zaman *et al*., 2008). This central role of glutamine and/or its derivatives in indicating nitrogen limitation seems to be evolutionarily conserved, occurring also in bacteria (Ikeda *et al*., 1996). Glutamine itself need not serve as the limiting species, however: another amino acid might instead (such as arginine, which also topped the ranked list). Dissecting the relative contributions of glutamine and its amino acid products to growth control will

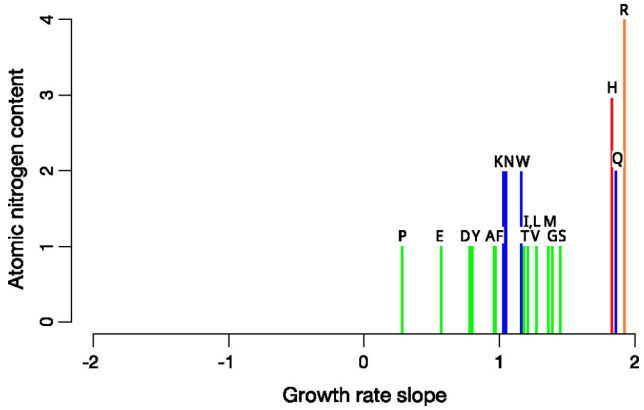

Figure 5. Growth rate slope for amino acids under nitrogen limitation. The positive growth rate slope found for every amino acid implies that, under nitrogen limitation, each amino acid's intracellular concentration increases with faster cellular growth rate (i.e., with partial relief of the nitrogen limitation). Amino acids are abbreviated by standard single-letter code.

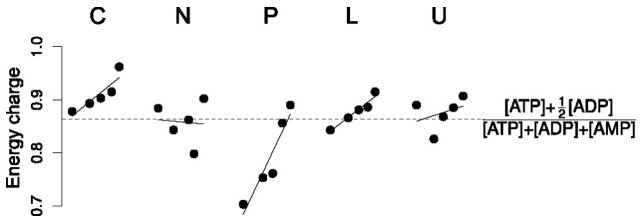

Figure 6. Adenylate energy charge across conditions and growth rates. Conventions are as per Figure 2: limiting nutrients are C, limitation for the carbon source, glucose; N, limitation for the nitrogen source, ammonium; P, limitation for the phosphorus source, phosphate; L, limitation for leucine in a leucine auxotroph; and U, limitation for uracil in a uracil auxotroph. Within each condition, steady-state growth rate increases from left to right from 0.05 to 0.3 h^{-1}. Black circles represent the median of N = 4 independent samples from each chemostat. Absolute intracellular concentrations of ATP, ADP, AMP, and adenosine were ~2.7, 0.6, 1.0, and 0.2 mM in the slowest-growing phosphorus-limited chemostats and 13, 0.8, 1.4, and 0.002 mM in the slowest-growing carbon-limited chemostats. Absolute concentrations in other conditions can be calculated from these values and the relative concentration data provided in Supplemental Dataset 1.

require additional experiments, e.g., direct measurement of tRNA loading, examination of strains with altered expression of amino acid biosynthetic enzymes or tRNAs.

Growth-limiting Species in Phosphorus (Phosphate) Limitation

The principal reaction of phosphate assimilation is phosphorylation of ADP to ATP. During phosphate limitation, ATP was identified as a potential growth-limiting species (Figures 2 and 4B and Table 1). Low levels of ATP can affect a great number of reactions, and a variety of direct and indirect products of ATP also showed growth-limiting patterns. These included NAD^+, UDP-glucose, and various sugar-phosphates, as well as UTP and CTP (but interestingly not GTP, which may play a greater regulatory role in bacteria; see, e.g., Krasny and Gourse, 2004).

Among these species, the nucleotide triphosphates are the most directly related to biopolymer synthesis and thus particular appealing candidates to be growth limiting. Between ATP, UTP, and CTP, genetic evidence points to ATP being the most likely intracellular signal of phosphate status: two enzymes of ATP metabolism, adenylate kinase and adenosine kinase, negatively regulate the PHO pathway (Auesukaree *et al*., 2005; Huang and O'Shea 2005). One of these, adenylate kinase, catalyzes the conversion of two ADP molecules into ATP and AMP and thus serves to maintain cellular ATP levels.

During phosphorus limitation, when ATP was strongly decreased, ADP fell only slightly and AMP accumulated. Adenylate energy charge (AEC), defined as follows:

$$AEC = ([ATP] + 0.5\,[ADP])/([ATP] + [ADP] + [AMP]) \quad (3)$$

strongly fell (Figure 6). It is unclear, however, whether the cells were actually energy limited, as the free energy of ATP hydrolysis differs from adenylate energy charge in being sensitive to the concentration of free P_i but not [AMP]:

$$\triangle G = \triangle G^{o'} + RT \ln ([ADP][P_i]/[ATP]) \quad (4)$$

As the concentration of free phosphate in the cell is presumably very low during phosphorus limitation, it is likely that the cells maintained a relatively constant free energy of ATP hydrolysis despite their putative low adenylate energy charge. In contrast, during carbon (glucose) limitation, where energy availability might be expected to limit growth, adenylate energy charge remained high. Other stimuli that block energy production, however, such as sudden shift of respiring yeast to anaerobic conditions (Abbott *et al*., 2009), or iron depletion (Thomas and Dawson 1977), do alter energy charge. Accordingly, although "adenylate energy charge" indeed sometimes reflects energy-generating capabilities, it is also a measure of phosphorus charge.

Growth-limiting Species in Carbon (Glucose) Limitation

As noted above, we did not observe a decrease in ATP or a large drop in adenylate energy charge during carbon (glucose) limitation (Figures 1, 2, and 6). Similar results have previously been obtained in *Escherichia coli* fed different carbon sources (Schneider and Gourse 2004). Moreover, in yeast, acute relief of glucose limitation depletes, rather than increases, ATP levels (Somsen *et al*., 2000). Thus, we suggest that, at least under aerobic conditions, glucose limitation leads to intracellular limitation for carbon, not energy.

In addition to signaling nitrogen limitation, depletion of amino acids is a possible reflection of carbon limitation. Two amino acids, threonine and arginine, showed a growth-limiting pattern (Figure 4C), with threonine more sensitive to carbon than nitrogen availability. Histidine, although just missing the statistical cut-off for being growth limiting in glucose, showed a similar pattern to arginine, and these two amino acids cluster tightly together in Figure 1. Interestingly, histidine biosynthesis is intertwined with purine biosynthesis, whereas arginine is intertwined with that of pyrimidines. It is accordingly possible that the depletion of these amino acids during nitrogen and carbon limitation plays a role in maintaining nucleotide pools when either carbon or nitrogen is scarce (e.g., by leading to impairment of protein synthesis and thereby decreased RNA synthesis).

Other metabolites showing a growth-limiting pattern in carbon (glucose) limitation included dihydroxyacetone phosphate and *N*-acetyl-glucosamine-1-phosphate, both of which were also low in phosphorus limitation. Dihydroxyacetone phosphate is a key glycolytic intermediate. N-acetyl-glucosamine-1-phosphate is a precursor to UDP-*N*-acetyl-glucosamine, a substrate in protein glycosylation and chitin biosynthesis. Although UDP-*N*-acetyl-glucosamine did not show a growth-limiting pattern, the identification of such a pattern in *N*-acetyl-glucosamine-1-phosphate is intriguing, as a closely related pathway in *Bacillus subtilis* was recently implicated in nutrient control of cell size (Weart *et al*., 2007). Moreover, chitin localizes to the yeast bud, a location especially relevant to cell division (Cabib and Bowers 1971).

Pyruvate, which topped the list of potential intracellular indicators of glucose limitation (Table 1), was more specifically depleted in glucose limitation. Although pyruvate is not a direct biopolymer precursor, it does play a critical role in setting the balance between fermentation and respiration. Pyruvate dehydrogenase, which leads to acetyl-CoA and respiration, has a higher affinity for pyruvate than pyruvate decarboxylase, which leads to fermentative ethanol production. Low concentrations of pyruvate therefore favor respiration (Kresze and Ronft 1981; Postma *et al*., 1989; Nalecz *et al*., 1991; Pronk *et al*., 1996). Consistent with this, the glucose-limited cultures at low dilution rates, where no ethanol was produced (Supplemental Figure S6), had the lowest pyruvate concentrations across all conditions. In contrast, the fastest growing of the glucose-limited chemostats, where ethanol secretion occurred, had substantially higher pyru-

vate. The switch from respiratory to respiro-fermentative growth was accompanied by a sharp drop in biomass, as expected based on previous literature (Supplemental Figure S7) (Barford and Hall 1979; Avigad 1981; Postma *et al*., 1989; Moore *et al*., 1991; Goncalves *et al*., 1997).

A Simple Quantitative Model of Growth Control

The above-mentioned analysis identified intracellular metabolites whose depletion might hinder cellular growth during nutrient limitation. A simplified model for this process involves envisioning growth as the assembly of these critical metabolites into biopolymer. The rate of growth could then be approximated as a maximum rate, which decreases whenever any of the critical components is scarce:

$$\mu = \frac{\mu_{\max}}{\sum_n \left(1 + \frac{k_n}{x_n}\right)} + \varepsilon, n \in \{C, N, P, U\} \quad (5)$$

where μ is the growth rate, $\mu_{\max}$ the maximum growth rate in the absence of nutrient limitation, x_n the concentrations of the limiting intracellular metabolite associated with nutrient limitation n, and k_n the K_m for x_n. To test this model, we selected pyruvate, glutamine, ATP, and UTP as the putative limiting intracellular metabolites in carbon (C), nitrogen (N), phosphorus (P), and uracil (U) limitation, respectively. These selections are based on the particularly significant depletion of these species in the relevant nutrient condition (Table 1), their clear connection to the limiting nutrient, and their involvement (with the exception of pyruvate) in RNA or protein synthesis. The model did not consider leucine limitation, as leucine was not differentiated from isoleucine in our analyses. The model, using data from only four metabolites, fit the experimental data well (cross-validated R^2 of 0.75, $p = 3 \times 10^{-7}$). Importantly, this good fit did not require selective sensing of specific metabolites in particular nutrient conditions, but the more physically realistic case where all potential limiting species interact to control growth rate.

Overflow Metabolites

Although not candidates to limit growth, metabolites that accumulate during nutrient limitation are also informative regarding metabolic regulation. Early evidence for feedback inhibition in metabolic regulation came from the observation that pyrimidine intermediates accumulate during uracil limitation of a pyrimidine auxotroph (Pardee and Yates 1956). Here, we recapitulate this finding, with dihydroorotate and orotate levels highest in severely pyrimidine-limited cells. It is possible that these high intermediate levels, not just decreased levels of end products, may adversely impact growth rate.

In leucine limitation, although we did not measure any pathway intermediates, we found a large number of other metabolites whose levels were elevated, including most amino acids (Figure 1). When growth is slowed due to an auxotrophic limitation, if feedback inhibition is the main means of regulation, all metabolic end products unrelated to the auxotrophy are expected to accumulate. Quantitative analysis (see Supplemental Material) suggests that the concentrations of these end products should be a function of growth rate but independent of the nature of the auxotrophy (as long as the auxotrophy is in a pathway separate from that producing the end product). Experimentally, however, amino acids accumulate much more strongly in leucine versus uracil limitation (Figure 1), pointing to the importance of other modes of regulation, e.g., general up-regulation of amino acid biosynthetic enzymes in leucine limitation due to Gcn4p activation (discussed below). In addition to amino acids, compounds accumulating in leucine limitation included phenylpyruvate, choline, glycerate, and pyruvate. The accumulation of pyruvate is consistent with the wasting of glucose that occurs when yeast are limited for an auxotrophic requirement but not for an elemental nutrient (Brauer *et al*., 2008). In addition, pyruvate provides the carbon skeleton for leucine biosynthesis.

In natural limitations, lack of availability of substrates (e.g., glutamine in nitrogen limitation, ATP in phosphorus limitation) may impair biosynthesis. Accordingly, overflow of end products was not predicted, and it did not generally occur (Figure 1). In nitrogen limitation, metabolites instead accumulated in the part of the TCA cycle directly upstream of ammonium assimilation (Figure 1). The accumulation of α-ketoglutarate presumably underlies similar accumulation of phenylpyruvate, which is linked to α-ketoglutarate by transamination. In nitrogen limitation, trehalose (which rose in concentration during slow growth in every nutrient condition) was present at particularly high levels. This may reflect cellular efforts to store carbon when growth is nitrogen limited (Lillie and Pringle 1980), or to compensate for decreased osmotic pressure when amino acid concentrations fall.

In phosphorus limitation, a large number of nucleosides and nitrogenous bases were found to overflow. These compounds are not involved in de novo nucleotide biosynthesis but instead are generated when phosphate moieties are scavenged from nucleotide monophosphates, e.g., via adenosine kinase, whose knockout favors activation of the PHO pathway (Auesukaree *et al*., 2005; Huang and O'Shea 2005). The overflow also of pyrimidine nucleosides and bases argues that, in addition to its annotated activity as a pyrimidine salvage enzyme, uridine kinase can function as a phosphate scavenge enzyme. Interestingly, glycerate and choline, two compounds that overflowed for unknown reasons during leucine limitation, also did so during phosphorus limitation. One possibility is that the overflow of choline (and possibly glycerate) indicates increased recycling of phospholipids: phosphatidylcholine can be deacylated by *NTE1*, yielding glycerophosphocholine (Zaccheo *et al*., 2004), which can subsequently be used by *S. cerevisiae* as a phosphate source (Fernández-Murray and McMaster, 2005).

Although essentially all cellular metabolites contain carbon, glucose limitation nevertheless resulted in the significant accumulation (i.e., positive nutrient mean effect) of certain species: mainly, multiply phosphorylated nucleotides such as triphosphates, UDP-glucose, and NAD^+ (Figure 1). Among these, the abundance of NAD^+ also significantly decreased with faster growth, meeting our criteria for overflow (Figure 4C). The accumulation of NAD^+ when glucose is low may favor efficient respiration. In addition to nucleotide derivatives, glutamate, and its downstream product, proline, tended to rise in glucose limitation (Figures 1 and 4C). The accumulation of glutamate and proline was surprising, given that most amino acids levels were decreased in carbon limitation. It is possible that elevated glutamate in severely glucose-limited cells reflects an overabundance of nitrogen relative to carbon, which in turn may drive the reductive amination of α-ketoglutarate.

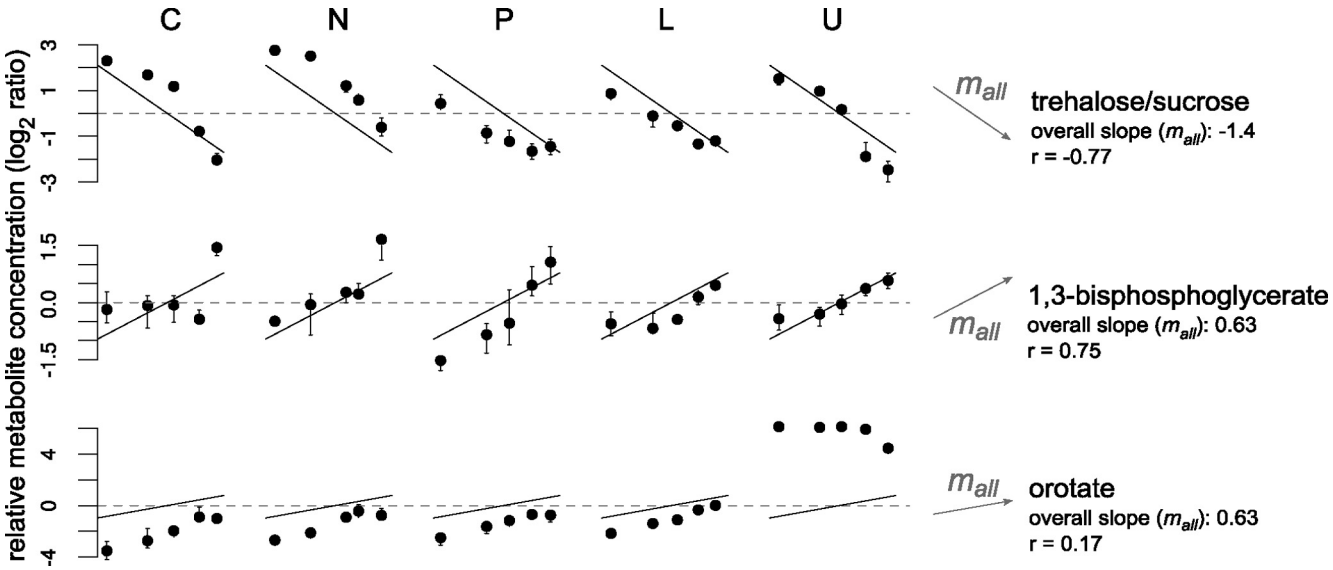

Figure 7. Metabolites with consistent growth rate responses across conditions. Conventions are as per Figure 2: limiting nutrients are C, limitation for the carbon source, glucose; N, limitation for the nitrogen source, ammonium; P, limitation for the phosphorus source, phosphate; L, limitation for leucine in a leucine auxotroph; and U, limitation for uracil in a uracil auxotroph. Within each condition, steady-state growth rate increases from left to right from 0.05 to 0.3 h^{-1}. Metabolites were fit to the single-parameter model in Eq. 6, with m_{all} representing the overall growth rate slope. The r values indicate goodness of fit. Note that orotate concentrations consistently increase with faster growth except under uracil limitation, where the knockout of *URA3* causes the buildup of orotate.

Metabolites Correlated to Growth Rate across Different Nutrients

Although the concentrations of most metabolites were highly dependent on the limiting nutrient, some metabolites did show a general trend to increase or decrease with growth rate (Figure 7 and Table 2). Metabolites whose abundance was strongly correlated with growth rate, irrespective of nutrient limitation, were identified on the basis of their goodness-of-fit (r) to an analogue of Eq. 2 with all nutrient-specific terms removed:

$$\log([M]_{n,\mu}/[M]_0) = m_{overall} \log(\mu/\mu_0) \quad (6)$$

Metabolites showing a statistically significant positive growth rate slope across all nutrient conditions (Bonferroni–Holm corrected p value <0.05, which corresponded to $r > 0.64$) included the lower glycolytic intermediates dihydroxyacetone-phosphate and bisphosphoglycerate and the nucleotide precursor ribose phosphate. When we considered only natural limitation conditions, taking the same goodness-of-fit cut-off, we found that two pyrimidine intermediates (orotate and dihydroorotate) and the arginine biosynthetic intermediate argininosuccinate also increased significantly with growth rate.

The tendency for the glycolytic intermediates to increase with faster growth may reflect the rate of glucose metabolism being adjusted to meet growth requirements. Similarly, the concentrations of pyrimidine intermediates may relate to de novo pyrimidine biosynthetic flux, argininosuccinate to de novo arginine biosynthesis, and ribose phosphate to overall nucleotide biosynthetic activity. In each case, the

Table 2. Metabolites whose abundance varies with growth rate regardless of the limiting nutrient

Condition tested	Behavior	Metabolite name	r
All limitations	Increasing	Bisphosphoglycerate	0.75
		Ribose-phosphate	0.70
		Dihydroxyacetone-phosphate	0.65
	Decreasing	Trehalose	−0.77
		Glutathione disulfide	−0.64
Only natural limitations	Increasing	Orotate	0.89
		Bisphosphoglycerate	0.75
		Dihydroorotate	0.74
		Argininosuccinate	0.71
		Ribose-phosphate	0.71
		Dihydroxyacetone-phosphate	0.66
	Decreasing	Trehalose	−0.73

Metabolite concentrations were fit to Eq. 6 by using either all five nutrient limitations, or by using only the natural conditions (carbon, nitrogen, and phosphorus); r values reflect goodness-of-fit, with the r cut-off of 0.64 corresponding to a Bonferroni–Holm corrected p value of 0.05.

higher intermediate concentrations may play a role in driving flux: for unsaturated enzymes, flux increases linearly with increasing metabolite concentrations. Thus, increasing concentrations of pyrimidine intermediates could drive biosynthesis without requiring increased synthesis of the corresponding enzymes. As we measured only a few biosynthetic intermediates outside of the pyrimidine pathway, other pathway intermediates may also increase with growth rate in a nutrient-nonspecific manner.

Only two metabolites showed a statistically significant trend to decrease with faster growth rate: trehalose and glutathione disulfide (Table 2) (the reduced form of glutathione also displayed a similar trend, with a Bonferroni–Holm corrected p value of 0.12.) Both trehalose and glutathione are produced by enzymes that are targets of the Msn2p and Msn4p transcription factors, whose activities increase with slower cell growth. Of these two metabolites, trehalose concentrations were most tightly correlated to growth rate (Table 2). This observation is consistent with trehalose biosynthesis and utilization being temporally compartmentalized within the cell cycle, with synthesis occurring in G1 and use in S phase (Kuenzi and Fiechter 1969; Paalman *et al*., 2003; Tu *et al*., 2005, 2007). As faster growth involves a shortening of G1 but not S phase (Hartwell *et al*., 1974; Unger and Hartwell 1976), the concentration of trehalose should decrease as the growth rate increases, as we observed. The accumulation of trehalose during the G1 phase may contribute to cell cycle control, with burning of trehalose helping to drive nutrient-limited cells through "Start", the entry point of the yeast cell division cycle (Futcher 2006). A possible benefit of this arrangement would be that cells would pass Start only when adequate internal carbon sources were available to make it back to G1, thereby protecting cells from being stranded in the cell cycle if environmental nutrient availability were to dry up (Chen *et al*., 2007).

Previously, it was observed that transcripts up-regulated with faster growth tended to be involved in biosynthesis and protein translation, whereas down-regulated transcripts were enriched for genes that play a role in the stress response (Brauer *et al*., 2008). An increase in trehalose has been suggested to be protective in osmotic stress (Hounsa *et al*., 1998) and heat shock (Singer and Lindquist, 1998), and glutathione plays a central role in the response to oxidative stress (reviewed in Penninckx, 2002). This suggests that "biosynthetic" metabolites may increase while "stress-related" metabolites are depleted with faster growth, mirroring the functional classifications observed in the transcriptome.

Correlating Metabolite and Transcript Levels

Brauer *et al*. (2008) have reported transcript data under the same conditions that we have used in the current study. In analyzing these data, Brauer *et al*. (2008) focused on responses that were independent of the identity of the limiting nutrient. To find nutrient-specific responses, we determined the nutrient mean effect and growth rate slope for transcripts, resulting in analogous scatter plots to those in Figures 3 and 4 (for these plots, see http://growthrate.princeton.edu/metabolome/). The top left and bottom right quadrants of these plots have different meanings for transcripts than for metabolites. For transcripts, those most induced during nutrient limitation appear in the lower right quadrant, e.g., transporters expressed to cope with scarcity of their substrates. We term such transcripts "limitation induced." Those most repressed during nutrient limitation appear in the top left quadrant, and we term these transcripts "limitation repressed."

Compared with the measured metabolite abundances, substantially fewer transcripts (20% at an FDR of 0.1 vs. 38% of metabolites at the same cut-off) showed significant limitation-induced or -repressed patterns. Such transcripts were significantly enriched for genes with known metabolic functions: the Gene Ontology terms "nitrogen compound metabolic process," "metabolic process," "pentose metabolic process," "nucleoside, nucleotide, and nucleotide metabolic process," and "water-soluble vitamin metabolic process" were all significant at an FDR of 0.01. In general, the functions of these transcripts corresponded well to their expression patterns. For example, in nitrogen limitation, the genes encoding the high-affinity, but energy-inefficient, ammonium assimilation pathway GS-GOGAT (*GLN1* and *GLT1*) were induced. These genes are regulated by the transcription factors Gln3p and Gat1p, which are regulated by nitrogen availability through target of rapamycin (TOR) complex 1 (Coffman *et al*., 1996, 1997; Valenzuela *et al*., 1998).

Many genes involved in oxidative metabolism were induced in carbon (glucose) limitation, e.g., *ACS1*, *ADH2*, *CIT3*, *CTA1*, *POT1*, and *POX1*, all of which are regulated by the glucose sensitive transcription factor Adr1p (Young *et al*., 2003; Tachibana *et al*., 2005). In contrast, *HXK2* was repressed by glucose limitation, consistent with its being a major glucose kinase in high glucose conditions and a mediator of glucose repression (Ma and Botstein 1986; Diderich *et al*., 2001). Similarly, the high-affinity glucose transporters *HXT6* and *HXT7* were induced by glucose limitation, whereas the low and intermediate affinity transporters (*HXT1*, *HXT3*, and *HXT4*) were repressed (reviewed in Kruckeberg 1996; Boles and Hollenberg 1997).

Targets of the Leu3p transcriptional regulator (Kohlhaw 2003; Boer *et al*., 2005) *LEU1*, *LEU4*, *OAC1*, *ILV2*, and *ILV3* were induced by leucine limitation, as were many genes regulated by Gcn4p, which activates transcription in response to uncharged tRNA (Hinnebusch 1992; Natarajan *et al*., 2001). Among genes with a positive nutrient mean effect in leucine limitation, 27% (49 of 182) were documented targets of Gcn4p (Teixeira *et al*., 2006), versus 9% of all measured genes, a significant enrichment ($p < 10^{-13}$ by Fisher's exact test). This induction of amino acid biosynthesis pathways under leucine limitation, when ample carbon and nitrogen were available, presumably accounts for the rampant amino acid accumulation in these cells (Figure 1).

In phosphorus limitation, one of the most striking transcriptional patterns was, intriguingly, not directly related to phosphate metabolism, but instead to sulfate. *SUL1*, *MMP1*, *MHT1*, *CYS3*, *MUP1*, and *SAM1* were strongly repressed by phosphorus limitation, with *SUL1* in phosphorus limitation showing the most positive growth rate slope of any gene in any condition. This suggests a strong relationship between phosphate limitation and sulfur metabolism. The repression of the high-affinity sulfate permease *SUL1* when phosphate is scarce (see also Tai *et al*., 2005), is probably a consequence of nonspecific sulfate transport through the highly expressed phosphate transporters. Nonspecific transport has been described previously for ammonium through potassium channels (Hess *et al*., 2006), where uncontrolled ammonium influx led the yeast to excrete amino acids in an effort to detoxify ammonia. Consistent with cells needing to decrease the intracellular concentration of free sulfate, in phosphorus limitation we observe modestly higher methionine and glutathione concentrations. Interestingly, clones isolated after prolonged phosphate limitation often display increased expression of sulfur assimilation pathways (Gre-

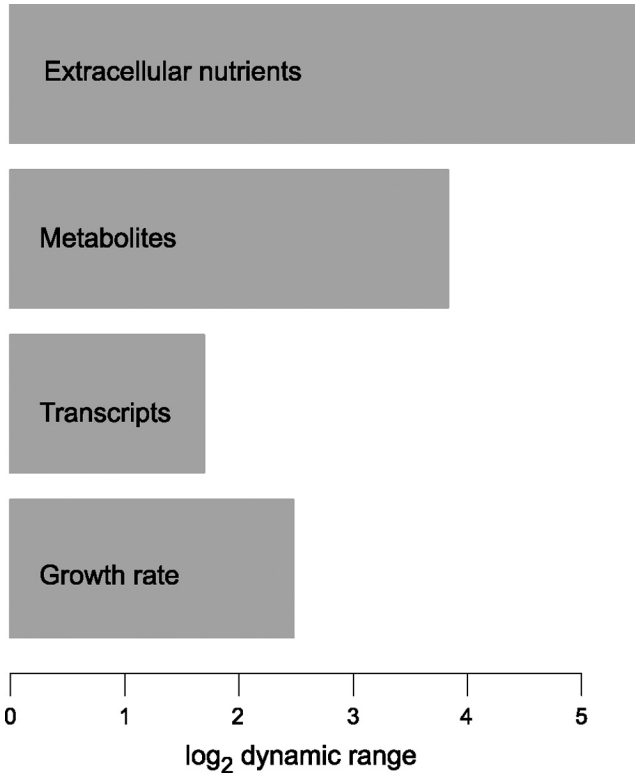

Figure 8. Dynamic range of extracellular and intracellular small molecules, transcripts, and cellular growth rate. Dynamic range refers to the maximum fold-change across all experiments. Reported values for nutrients, metabolites, and transcripts are the median across all measured species. For nutrients, the measured species are glucose (across all conditions), leucine (in leucine limitation), and uracil (in uracil limitation). Note that transcripts were measured by microarray; measurement by sequencing might yield a larger dynamic range.

sham *et al*., 2008). This would suggest that high intracellular sulfate (or a high intracellular ratio of sulfate to phosphate), resulting from the increased sulfate influx through phosphate transporters, is detrimental to yeast, which evolve the ability to more rapidly assimilate sulfate to deal with this toxicity.

Divergent Metabolome, Homeostatic Transcriptome

A striking feature of the metabolome response was the magnitude of the concentration changes (Figure 1). This partial breakdown of homeostasis is perhaps not unexpected, given the relatively direct connection of metabolites to environmental nutrients. Environmental nutrient concentrations are outside the realm of cellular control, and in our experiments, extracellular glucose concentrations varied from 0.1 to 118 mM across different chemostats, corresponding to an ~1000-fold range, whereas leucine (in leucine-limited cells) and uracil (in uracil-limited cells) varied over a more modest, but still large range (~40-fold) (Supplemental Table S3). The median metabolite concentration also varied over a large range (14-fold) but not as large as the nutrients. In contrast, the median transcript varied over a substantially smaller range (3.2-fold), comparable with the experimental range of growth rates (5.5-fold). Thus, cellular regulatory systems partially dampen environmental variability at the level of the metabolome, and more strongly at the level of the transcriptome (Figure 8).

For metabolic enzymes, a key objective of transcriptional regulation is to control, via enzyme concentrations, metabolic flux. Although we did not measure metabolic flux here, in the absence of futile cycling, many fluxes are expected to scale linearly with growth rate. In this light, it is sensible that the experimental range of transcripts and growth rate are similar. Nevertheless, in preliminary efforts to relate enzyme expression to growth rate, we find many complexities. For example, enzymes catalyzing different steps in linear biosynthetic pathways sometimes show opposing patterns of regulation. These observations point to the importance of other modes of metabolic regulation, such as active site competition, allostery, and enzyme covalent modification, which require further dissection (see, e.g., Yuan *et al*., 2009). In such efforts, the existence of a consensus reconstruction of yeast metabolism will provide a valuable roadmap (Herrgård *et al*., 2008).

Another important question is how regulatory systems ultimately link the metabolome to growth rate and the transcriptome. The most straightforward possibility is that metabolite availability directly controls growth rate by limiting the availability of substrates for biomass synthesis. Such a view is consistent with the ability of cells to tailor their growth rate to auxotrophic requirements, and with our ability to model growth rate using a simple Michaelis-Menten approach based on a few limiting nutrients. Hence an appealing possibility is that the expression of transcripts showing generic growth rate effects is regulated downstream of growth rate, rather than solely via integration of signals from various nutrient-specific sensing pathways, including Ras/protein kinase A for glucose, TOR complex 1 for nitrogen and Pho80/Pho85 for phosphate (reviewed in Zaman *et al*., 2008). This possibility would account for the similarity between the transcriptional responses to auxotrophic and to natural nutrient limitations, even when no system for sensing the auxotrophic limitation exists. One potential means by which transcription could be directly controlled by growth rate involves steady production of a transcriptional activator or repressor (at a rate independent of growth rate), with the intracellular concentration of that activator or repressor controlled by dilution by cell growth. Another possibility is that the total rates of protein and/or RNA synthesis might be sensed by the cell.

In addition to the nature of the mechanism linking the metabolome to the transcriptome, the precise pathway by which nutrient limitation controls growth also requires further investigation. One issue is whether the limiting intracellular metabolites actually fall to levels that directly limit biosynthesis, or instead just to levels that alter the activity of nutrient-sensing systems such as TOR. Another issue is that each elemental nutrient limitation resulted in decreases in the concentrations of multiple possible growth-limiting metabolites. This observation contrasts with a theoretical expectation that only a single metabolite should be growth limiting at any instant, as, even if the production of many metabolites is slowed by insufficient nutrient concentrations, only the one whose production is impaired the most will be limiting (Wingreen and Goyal, personal communication). Even though many species fall in concentration in each elemental nutrient limitation, it is possible that only a single species actually falls to limiting levels (e.g., in nitrogen limitation, glutamine might be growth limiting, with the fall in histidine, arginine, and other amino acids essentially incidental). More complex scenarios are also possible, however. One involves the limiting species varying between cells depending on inter-cell variation in enzyme expression. To this end, single-cell measurement of specific metabolite con-

centrations over time would be a valuable advance (Deuschle *et al*., 2005). Combined with genetic perturbations and direct measurement of tRNA loading, such experiments hold the promise to assemble the candidate limiting metabolites found here into well-validated growth-control pathways.

ACKNOWLEDGMENTS

We thank John Storey, Olga Troyanskaya, Edo Airoldi, and members of the Rabinowitz, Botstein, and Troyanskaya groups for helpful discussions. This work was funded by National Science Foundation CAREER award MCB-0643859 and Beckman Foundation and American Heart Association Awards (to J.D.R.); National Institutes of Health grant R01 GM-046406 (to D. B.), and the National Institute of General Medical Sciences Center for Quantitative Biology/National Institutes of Health grant P50 GM-071508.

REFERENCES

Abbott, D. A., van den Brink, J., Minneboo, I. M., Pronk, J. T., and van Maris, A. J. Anaerobic homolactate fermentation with *Saccharomyces cerevisiae* results in depletion of ATP and impaired metabolic activity. (2009). FEMS Yeast Res. *9*, 349–357.

Auesukaree, C., Tochio, H., Shirakawa, M., Kaneko, Y., and Harashima, S. (2005). Plc1p, Arg82p, and Kcs1p, enzymes involved in inositol pyrophosphate synthesis, are essential for phosphate regulation and polyphosphate accumulation in *Saccharomyces cerevisiae*. J. Biol. Chem. *280*, 25127–25133.

Avigad, G. (1981). Stimulation of yeast phosphofructokinase activity by fructose 2,6-bisphosphate. Biochemical and biophysical research communications *102*, 7.

Bajad, S. U., Lu, W., Kimball, E. H., Yuan, J., Peterson, C., and Rabinowitz, J. D. (2006). Separation and quantitation of water soluble cellular metabolites by hydrophilic interaction chromatography—tandem mass spectrometry. J. Chromatogr. A. *1125*, 76–88.

Barford, J. P., and Hall, R. J. (1979). Investigation of the significance of a carbon and redox balance to the measurement of gaseous metabolism of *Saccharomyces cerevisiae*. Biotechnol. Bioeng. *21*, 609–626.

Beck, C., and von Meyenburg, H. K. (1968). Enzyme pattern and aerobic growth of *Saccharomyces cerevisiae* under various degrees of glucose limitation. J. Bacteriol. *96*, 479–486.

Benjamini, Y., and Hochberg, Y. (1995). Controlling the false discovery rate: a practical and powerful approach to multiple testing. J. R. Stat. Soc. Ser. B Stat. Methodol. *1*, 289–300.

Bennett, B. D., Yuan, J., Kimball, E. H., and Rabinowitz, J. D. (2008). Absolute quantitation of intracellular metabolite concentrations by an isotope ratio-based approach. Nat. Protoc. *3*, 1328–1340.

Boer, V. M., de Winde, J. H., Pronk, J. T., and Piper, M. D. (2003). The genome-wide transcriptional responses of *Saccharomyces cerevisiae* grown on glucose in aerobic chemostat cultures limited for carbon, nitrogen, phosphorus, or sulfur. J. Biol. Chem. *278*, 3265–3274.

Boer, V. M., Daran, J. M., Almering, M. J., de Winde, J. H., and Pronk, J. T. (2005). Contribution of the *Saccharomyces cerevisiae* transcriptional regulator Leu3p to physiology and gene expression in nitrogen- and carbon-limited chemostat cultures. FEMS Yeast Res. *5*, 885–897.

Boles, E., and Hollenberg, C. P. (1997). The molecular genetics of hexose transport in yeasts. FEMS Microbiol. Rev. *21*, 85–111.

Brauer, M. J., Huttenhower, C., Airoldi, E. M., Rosenstein, R., Matese, J. C., Gresham, D., Boer, V. M., Troyanskaya, O. G., and Botstein, D. (2008). Coordination of growth rate, cell cycle, stress response, and metabolic activity in yeast. Mol. Biol. Cell *19*, 352–367.

Cabib, E., and Bowers, B. (1971). Chitin and yeast budding. Localization of chitin in yeast bud scars. J. Biol. Chem. *246*, 152–159.

Castrillo, J. I., *et al*. (2007). Growth control of the eukaryote cell: a systems biology study in yeast. J. Biol. *6*, 4.

Chen, Z., Odstrcil, E. A., Tu, B. P., and McKnight, S. L. (2007). Restriction of DNA replication to the reductive phase of the metabolic cycle protects genome integrity. Science *316*, 1916–1919.

Coffman, J. A., Rai, R., Cunningham, T., Svetlov, V., and Cooper, T. G. (1996). Gat1p, a GATA family protein whose production is sensitive to nitrogen catabolite repression, participates in transcriptional activation of nitrogen-catabolic genes in *Saccharomyces cerevisiae*. Mol. Cell Biol. *16*, 847–858.

Coffman, J. A., Rai, R., Loprete, D. M., Cunningham, T., Svetlov, V., and Cooper, T. G. (1997). Cross regulation of four GATA factors that control nitrogen catabolic gene expression in *Saccharomyces cerevisiae*. J. Bacteriol. *179*, 3416–3429.

Cooney, C. L., and Wang, D. I. (1976) Transient response of *Enterobacter* aerogenes under a dual nutrient limitation in a chemostat. Biotechnol. Bioeng. *18*, 189–198.

Crespo, J. L., Powers, T., Fowler, B., and Hall, M. N. (2002). The TOR-controlled transcription activators GLN3, RTG1, and RTG3 are regulated in response to intracellular levels of glutamine. Proc. Natl. Acad. Sci. USA *99*, 6784–6789.

de Koning, W., and van Dam, K. (1992). A method for the determination of changes of glycolytic metabolites in yeast on a subsecond time scale using extraction at neutral pH. Anal. Biochem. *204*, 118–123.

Deuschle, K., Okumoto, S., Fehr, M., Looger, L. L., Kozhukh, L., and Frommer, W. B. (2005). Construction and optimization of a family of genetically encoded metabolite sensors by semirational protein engineering. Protein Sci. *14*, 2304–2314.

Diderich, J. A., Raamsdonk, L. M., Kruckeberg, A. L., Berden, J. A., and Van Dam, K. (2001). Physiological properties of *Saccharomyces cerevisiae* from which hexokinase II has been deleted. Appl. Environ. Microbiol. *67*, 1587–1593.

Eisen, M. B., Spellman, P. T., Brown, P. O., and Botstein, D. (1998). Cluster analysis and display of genome-wide expression patterns. Proc. Natl. Acad. Sci. USA *95*, 14863–14868.

Futcher, B. (2006). Metabolic cycle, cell cycle, and the finishing kick to Start. Genome Biol. *7*, 107.

Gasch, A. P., Spellman, P. T., Kao, C. M., Carmel-Harel, O., Eisen, M. B., Storz, G., Botstein, D., and Brown, P. O. (2000). Genomic expression programs in the response of yeast cells to environmental changes. Mol. Biol. Cell *11*, 4241–4257.

Goncalves, P. M., Griffioen, G., Bebelman, J. P., and Planta, R. J. (1997). Signalling pathways leading to transcriptional regulation of genes involved in the activation of glycolysis in yeast. Mol. Microbiol. *25*, 483–493.

Fernández-Murray, J. P., and McMaster, C. R. (2005). Glycerophosphocholine catabolism as a new route for choline formation for phosphatidylcholine synthesis by the Kennedy pathway. J. Biol. Chem. *280*, 38290–38296.

Gresham, D., Desai, M. M., Tucker, C. M., Jenq, H. T., Pai, D. A., Ward, A., DeSevo, C. G., Botstein, D., and Dunham, M. J. (2008) The repertoire and dynamics of evolutionary adaptations to controlled nutrient-limited environments in yeast. PLoS Genet. *4*, e1000303.

Hartwell, L. H., Culotti, J., Pringle, J. R., and Reid, B. J. (1974). Genetic control of the cell division cycle in yeast. Science *183*, 46–51.

Herrgård, M. J., *et al*. (2008). A consensus yeast metabolic network reconstruction obtained from a community approach to systems biology. Nat. Biotechnol. *26*, 1155–1160.

Hess, D. C., Lu, W., Rabinowitz, J. D., and Botstein, D. (2006). Ammonium toxicity and potassium limitation in yeast. PLoS Biol. *4*, e351.

Hinnebusch, A. G. (1992). General and pathway specific regulatory mechanisms controlling the synthesis of amino acid biosynthetic enzymes in *Saccharomyces cerevisiae*. The molecular and cellular biology of the yeast *Saccharomyces*: gene expression. Cold Spring Harbor, NY: Cold Spring Harbor Laboratory Press.

Hounsa, C., Brandt, E. V., Thevelein, J., Hohmann, S., and Prior, B. A. (1998). Role of trehalose in survival of *Saccharomyces cerevisiae* under osmotic stress. Microbiol. *144*, 671–680.

Huang, S., and O'Shea, E. K. (2005). A systematic high-throughput screen of a yeast deletion collection for mutants defective in PHO5 regulation. Genetics *169*, 1859–1871.

Ikeda, T. P., Shauger, A. E., and Kustu, S. (1996). Salmonella typhimurium apparently perceives external nitrogen limitation as internal glutamine limitation. J. Mol. Biol. *259*, 589–607.

Kohlhaw, G. B. (2003). Leucine biosynthesis in fungi: entering metabolism through the back door. Microbiol. Mol. Biol. Rev. *67*, 1–15, table of contents.

Kolkman, A., Daran-Lapujade, P., Fullaondo, A., Olsthoorn, M. M., Pronk, J. T., Slijper, M, and Heck, A. J. (2006). Proteome analysis of yeast response to various nutrient limitations. Mol. Syst. Biol. *2*, 2006.0026.

Krasny, L., and Gourse, R. L. (2004). An alternative strategy for bacterial ribosome synthesis: *Bacillus subtilis* rRNA transcriptional regulation. EMBO J. *23*, 4473.

Kresze, G. B., and Ronft, H. (1981). Pyruvate dehydrogenase complex from baker's yeast. 1. Purification and some kinetic and regulatory properties. Eur. J. Biochem. *119*, 573–579.

Kruckeberg, A. L. (1996). The hexose transporter family of *Saccharomyces cerevisiae*. Arch. Microbiol. *166*, 283–292.

Kuenzi, M. T., and Fiechter, A. (1969). Changes in carbohydrate composition and trehalase-activity during the budding cycle of *Saccharomyces cerevisiae*. Arch. Mikrobiol. *64*, 396–407.

Lillie, S. H., and Pringle, J. R. (1980). Reserve carbohydrate metabolism in *Saccharomyces cerevisiae*: responses to nutrient limitation. J. Bacteriol. *143*, 1384–1394.

Lu, W., Bennett, B. D., and Rabinowitz, J. D. (2008). Analytical strategies for LC-MS-based targeted metabolomics. J. Chromatogr. B Analyt. Technol. Biomed. Life Sci. *871*, 236–242.

Luo, B., Groenke, K., Takors, R., Wandrey, C., and Oldiges, M. (2007). Simultaneous determination of multiple intracellular metabolites in glycolysis, pentose phosphate pathway and tricarboxylic acid cycle by liquid chromatography-mass spectrometry. J. Chromatogr. A *1147*, 153–164.

Ma, H., and Botstein, D. (1986). Effects of null mutations in the hexokinase genes of *Saccharomyces cerevisiae* on catabolite repression. Mol. Cell Biol. *6*, 4046–4052.

Maharjan, R. P., and Ferenci, T. (2003). Global metabolite analysis: the influence of extraction methodology on metabolome profiles of *Escherichia coli*. Anal. Biochem. *313*, 145–154.

Mitchell, A. P., and Magasanik, B. (1984). Three regulatory systems control production of glutamine synthetase in *Saccharomyces cerevisiae*. Mol. Cell Biol. *4*, 2767–2773.

Monod, J. (1942). Recherches sur la Croissance des Cultures Bacteriennes, Paris, France: Hermann Cie.

Monod, J. (1950). La technique de culture continue, theorie et applications. Ann. Inst. Pasteur *79*, 390–410.

Moore, P. A., Sagliocco, F. A., Wood, R. M., and Brown, A. J. (1991). Yeast glycolytic mRNAs are differentially regulated. Mol. Cell Biol. *11*, 5330–5337.

Nalecz, M. J., Nalecz, K. A., and Azzi, A. (1991). Purification and functional characterisation of the pyruvate (monocarboxylate) carrier from baker's yeast mitochondria (*Saccharomyces cerevisiae*). Biochim. Biophys. Acta *1079*, 87–95.

Natarajan, K., Meyer, M. R., Jackson, B. M., Slade, D., Roberts, C., Hinnebusch, A. G., and Marton, M. J. (2001). Transcriptional profiling shows that Gcn4p is a master regulator of gene expression during amino acid starvation in yeast. Mol. Cell Biol. *21*, 4347–4368.

Novick, A., and Szilard, L. (1950). Description of the chemostat. Science *112*, 715–716.

Paalman, J. W., Verwaal, R., Slofstra, S. H., Verkleij, A. J., Boonstra, J., and Verrips, C. T. (2003). Trehalose and glycogen accumulation is related to the duration of the G1 phase of *Saccharomyces cerevisiae*. FEMS Yeast Res. *3*, 261–268.

Pardee, A. B., and Yates, R. A. (1956). Pyrimidine biosynthesis in *Escherichia coli*. J. Biol. Chem. *221*, 743–756.

Penninckx, M. J. (2002). An overview on glutathione in *Saccharomyces* versus non-conventional yeasts. FEMS Yeast Res. *2*, 295–305.

Pir, P., Kirdar, B., Hayes, A., Onsan, Z. I., Ulgen, K. O., and Oliver, S. G. (2008). Exometabolic and transcriptional response in relation to phenotype and gene copy number in respiration-related deletion mutants of *S. cerevisiae*. Yeast *25*, 661–672.

Postma, E., Verduyn, C., Scheffers, W. A., and Van Dijken, J. P. (1989). Enzymic analysis of the crabtree effect in glucose-limited chemostat cultures of *Saccharomyces cerevisiae*. Appl. Environ. Microbiol. *55*, 468–477.

Pronk, J. T. (2002). Auxotrophic yeast strains in fundamental and applied research. Appl. Environ. Microbiol. *68*, 2095–2100.

Pronk, J. T., Yde Steensma, H., and Van Dijken, J. P. (1996). Pyruvate metabolism in *Saccharomyces cerevisiae*. Yeast *12*, 1607–1633.

R Development Core Team (2008) R: A Language and Environment for Statistical Computing, Vienna, Austria: R Foundation for Statistical Computing.

Rabinowitz, J. D., and Kimball, E. (2007). Acidic acetonitrile for cellular metabolome extraction from *Escherichia coli*. Anal. Chem. *79*, 6167–6173.

Rhee, G. (1973). A continuous culture study of phosphate uptake, growth rate and polyphosphate in *Scenedesmus* sp. J. Phycol. *9*, 12.

Schneider, D. A., and Gourse, R. L. (2004). Relationship between growth rate and ATP concentration in *Escherichia coli*: a bioassay for available cellular ATP. J. Biol. Chem. *279*, 8262–8268.

Singer, M. A., and Lindquist, S. (1998). Multiple effects of trehalose on protein folding *in vitro* and *in vivo*. Mol. Cell *1*, 639–648.

Senn, H., Lendenmann, U., Snozzi, M., Hamer, G., and Egli, T. (1994). The growth of *Escherichia coli* in glucose-limited chemostat cultures: a re-examination of the kinetics. Biochim. Biophys. Acta *1201*, 424–436.

Somsen, O. J., Hoeben, M. A., Esgalhado, E., Snoep, J. L., Visser, D., van der Heijden, R. T., Heijnen, J. J., and Westerhoff, H. V. (2000). Glucose and the ATP paradox in yeast. Biochem. J. *352*, 593–599.

Tachibana, C., Yoo, J. Y., Tagne, J. B., Kacherovsky, N., Lee, T. I., and Young, E. T. (2005). Combined global localization analysis and transcriptome data identify genes that are directly coregulated by Adr1 and Cat8. Mol. Cell. Biol. *25*, 2138–2146.

Tai, S. L., Boer, V. M., Daran-Lapujade, P., Walsh, M. C., de Winde, J. H., Daran, J. M., and Pronk, J. T. (2005). Two-dimensional transcriptome analysis in chemostat cultures. Combinatorial effects of oxygen availability and macronutrient limitation in *Saccharomyces cerevisiae*. J. Biol. Chem. *280*, 437–447.

Teixeira, M. C., Monteiro, P., Jain, P., Tenreiro, S., Fernandes, A. R., Mira, N. P., Alenquer, M., Freitas, A. T., Oliveira, A. L., and Sá-Correia, I. (2006). The YEASTRACT database: a tool for the analysis of transcription regulatory associations in *Saccharomyces cerevisiae*. Nucleic Acids Res. *34*(Database issue), D446–D451.

Thomas, K. C., and Dawson, P. S. (1977). Variations in the adenylate energy charge during phased growth (cell cycle) of *Candida utilis* under energy excess and energy-limiting growth conditions. J. Bacteriol. *132*, 36–43.

Tu, B. P., Kudlicki, A., Rowicka, M., and McKnight, S. L. (2005). Logic of the yeast metabolic cycle: temporal compartmentalization of cellular processes. Science *310*, 1152–1158.

Tu, B. P., Mohler, R. E., Liu, J. C., Dombek, K. M., Young, E. T., Synovec, R. E., and McKnight, S. L. (2007). Cyclic changes in metabolic state during the life of a yeast cell. Proc. Natl. Acad. Sci. USA *104*, 16886–16891.

Unger, M. W., and Hartwell, L. H. (1976). Control of cell division in *Saccharomyces cerevisiae* by methionyl-tRNA. Proc. Natl. Acad. Sci. USA *73*, 1664–1668.

Valenzuela, L., Ballario, P., Aranda, C., Filetici, P., and Gonzalez, A. (1998). Regulation of expression of GLT1, the gene encoding glutamate synthase in *Saccharomyces cerevisiae*. J Bacteriol. *180*, 3533–3540.

Villas-Bôas, S. G., Højer-Pedersen, J., Akesson, M., Smedsgaard, J., and Nielsen, J. (2005). Global metabolite analysis of yeast: evaluation of sample preparation methods. Yeast *22*, 1155–1169.

Weart, R. B., Lee, A. H., Chien, A. C., Haeusser, D. P., Hill, N. S., and Levin, P. A. (2007). A metabolic sensor governing cell size in bacteria. Cell *130*, 335–347.

Winston, F., Dollard, C., and Ricupero-Hovasse, S. L. (1995). Construction of a set of convenient *Saccharomyces cerevisiae* strains that are isogenic to S288C. Yeast *11*, 53–55.

Wu, L., Mashego, M. R., van Dam, J. C., Proell, A. M., Vinke, J. L., Ras, C., van Winden, W. A., van Gulik, W. M., and Heijnen, J. J. (2005). Quantitative analysis of the microbial metabolome by isotope dilution mass spectrometry using uniformly 13C-labeled cell extracts as internal standards. Anal. Biochem. *336*, 164–171.

Young, E. T., Dombek, K. M., Tachibana, C., and Ideker, T. (2003). Multiple pathways are co-regulated by the protein kinase Snf1 and the transcription factors Adr1 and Cat8. J. Biol. Chem. *278*, 26146–26158.

Yuan, J., Doucette, C. D., Fowler, W. U., Feng, X. J., Piazza, M., Rabitz, H. A., Wingreen, N. S., and Rabinowitz, J. D. (2009). Metabolomics-driven quantitative analysis of ammonia assimilation in *E. coli*. Mol. Syst. Biol. *5*, 302.

Zaman, S., Lippman, S. I., Zhao, X., and Broach, J. R. (2008). How *Saccharomyces* responds to nutrients. Annu. Rev. Genet. *42*, 27–81.

Zaccheo, O., Dinsdale, D., Meacock, P. A., and Glynn, P. (2004). Neuropathy target esterase and its yeast homologue degrade phosphatidylcholine to glycerophosphocholine in living cells. J. Biol. Chem. *279*, 24024–24033.